Bioactive Constituents, Metabolites, and Functions

Lignans and Neolignans with Antioxidant and Human Cancer Cell Proliferation Inhibitory Activities from Cinnamomum bejolghota Confirm its Functional Food Property

Li Rao, Yun-Xia You, Yu Su, Yue Fan, Yu Liu, Qian He, Yi Chen, Jie Meng, Lin Hu, Yizhou Li, You-Kai Xu, Bin Lin, and Chuan-Rui Zhang

J. Agric. Food Chem., **Just Accepted Manuscript** • DOI: 10.1021/acs.jafc.0c02885 • Publication Date (Web): 27 Jul 2020

Lignans and Neolignans with Antioxidant and Human Cancer Cell Proliferation Inhibitory Activities from *Cinnamomum bejolghota* Confirm its Functional Food Property

Li Rao[†], Yun-Xia You[†], Yu Su[†], Yue Fan[†], Yu Liu[†], Qian He[†], Yi Chen[†], Jie Meng[†], Lin Hu[†], Yizhou Li[†], You-Kai Xu[‡], Bin Lin[§], Chuan-Rui Zhang*[,†,⊥]

[†]Chongqing Key Laboratory of Natural Product Synthesis and Drug Research, and Chemical Biology Research Center, School of Pharmaceutical Sciences, Chongqing University, Chongqing 401331, P. R. China

[‡]Key Laboratory of Tropical Plant Resource and Sustainable Use, Xishuangbanna Tropical Botanical Garden, Chinese Academy of Sciences, Menglun 666303, P. R. China

[§]School of Pharmaceutical Engineering, Shenyang Pharmaceutical University, Shenyang 110016, P. R. China

[⊥]State Key Laboratory of Natural Medicines, China Pharmaceutical University, Nanjing 210009, P. R. China

ABSTRACT:

In the aim to evaluate the functional food property of *Cinnamomum bejolghota*, seven new lignans and neolignans, bejolghotins A–G (**1**–**4** and **9**–**11**), along with 14 known ones (**5**–**8** and **12**–**21**), were isolated and their structures including absolute configurations were elucidated by extensive spectroscopic data and electronic circular dichroism analyses. All the isolates were tested for antioxidant and human cancer cell proliferation inhibitory activities. 20 compounds showed comparable antioxidant activity to the positive controls, and 3 ones significantly inhibited the growth of three cancer cell lines HCT-116, A549 and MDA-MB-231 with IC_{50} values of 0.78–2.93 μM, which confirmed its health benefits.

KEYWORDS: *Cinnamomum bejolghota*, lignans, neolignans, antioxidant activity, human cancer cell proliferation inhibition

INTRODUCTION

The genus *Cinnamomum*, one of the largest genera of Lauraceae, contained about 250 species distributed in tropical and subtropical Asia, Australia, and Pacific islands.[1] Many *Cinnamomum* species are grown in commerce with high economic value. Amongst, the most well-known species are *C. zeylanicum* and *C. cassia* with their bark (especially inner bark, also called cinnamon), leaves and essential oils are widely used for spices and condiments in food, including bakery, desserts cuisines and drinks,[2–8] such as cinnamon rolls served commonly in Northern Europe and North America. Plenty of studies about the volatile oils distilled from the various parts of plants in *Cinnamomum* genus have been carried out, which resulted in the report of a large number of natural products such as sesquiterpenoids[3,4,9–13], monoterpenoids[3,4,9,10,12,13] and phenylpropanoids[2–4,10–13] with diverse biological activities including antiinflammatory[2,9], antityrosinase[10], hepatoprotective[11], antioxidant[3,4,12] and hypoglycemic activities[13]. In addition, many *Cinnamomum* species have been also used as traditional medicines worldwidely, and phytochemical investigations on them have led to the discovery of a series of secondary metabolites such as butanolides[14,15], phenolic compounds[5,16,17], sesquiterpenoids[8,18], diterpenoids[7,19,20], neolignans[5,21,22], lignans[22] and flavonoids[5,6,22] with diverse bioactivities, including antioxidant[5], antimicrobial[8], antimigratory[14], tyrosinase-inhibitory[17], cytotoxic[14,15,18], immunostimulative[7,19,20], antiinflammatory[6,21] and neuroprotective[22] activities.

Cinnamomum bejolghota (Buch.-Ham.) Sweet, a small- to large-sized evergreen tree, distributed widely in South China and Southeast Asia.[1] It's worthy to note that its leaves, bark and panicle are all aromatic. It's also called as indigenous cinnamon, false cinnamon or mountain cinnamon and its barks have been used as spices in China.[1] In India, it had different local names like "Pati-Hunda", "Naga-dalchini", "Seerang-esing", "Sami-jong" and "Tejpat-manbi".[23] Also,

its barks were sold at the local markets and used as traditional spices in some region, while its leaves were used for preparing a kind of rice-beer called "Apong" in some ethnic societies.[23,24] On the other hand, it has been used as a medicinal plant for treating cough, cold, toothache and liver complaints.[23,25] Similarly, the essential oils of the leaves, bark, flower and panicle of *C. bejolghota* have been investigated by GC and GC/MS,[23,24] along with their antihyperglycemic, antibacterial and antifungal activities.[25,26] Except of those essential oil studies and very limited preliminary pharmacognostic evaluation on its bark collected from India, there were no any reports about the detailed nonvolatile components and their bioactivities of this plant. In this study the leaves and twigs of *C. bejolghota* were investigated to evaluate its chemical constituents by using in vitro antioxidant and human cancer cell proliferation inhibitory bioassays, which resulted in the isolation and characterization of seven new (**1**−**4** and **9**−**11**) and fourteen known (**5**−**8** and **12**−**21**) lignans and neolignans. 20 compounds showed comparable antioxidant activity to the positive controls in DPPH assay and 6 ones displayed human cancer cell proliferation inhibition against three cancer cell lines including 3 ones with strong activity comparable to the positive control. This was the first time to report the isolation of chemical constituents from *C. bejolghota* and this study confirmed its functional food property.

MATERIALS AND METHODS

Safety. There were no safety concerns associated with this study.

General Experimental Procedures. Optical rotations were measured with a Rudolph Autopol I automatic polarimeter. UV spectra were measured using an Agilent Cary60 spectrophotometer. IR spectra were obtained on a Bruker TENSOR 27 spectrometer using KBr disks. NMR spectra were performed on an Agilent DD2 600 MHz instrument. Semi-preparative HPLC was performed on a Waters 1525 pump equipped with a Waters 2489 detector and an

YMC-pack ODS-A column (10 × 250 mm, S-5 μm, 12 nm). HRESIMS were recorded on a Bruker SolariX 7.0T instrument. Column chromatography (CC) was performed using silica gel (200-300 mesh, Qingdao Haiyang Chemical Co., Ltd.), MCI gel (CHP20P, 75-150 μm, Mitsubishi Chemical Industries Ltd.) and Sephadex LH-20 (Amersham Biosciences, Sweden). Thin-layer chromatography (TLC) was conducted on silica gel 60 GF254 plates (Qingdao Haiyang Chemical Co., Ltd.). All solvents used were purchased from Cheng Du Chron Chemicals Co., Ltd. 3-(4,5-dimethylthiazole-2-yl)-2,5-diphenyltetrazolium bromide (MTT), 1,1-Diphenyl-2-picrylhydrazine (DPPH), L-ascorbic acid and butylatedhydroxytoluene (BHT) were purchased from Sigma-Aldrich Chemical Company (St. Louis, MO). Fetal bovine serum (FBS) and DMEM (Hyclone) medium were purchased from Gibco BRL (Grand Island, NY, USA). Human cancer cell lines HCT-116 (colon), MDA-MB-231 (breast) and A549 (lung), and human normal cell lines BEAS-2B and L02 were purchased from Shanghai Cell bank of Chinese Academy of Sciences (Shanghai, China).

Plant Material. The leaves and twigs of *Cinnamomum bejolghota* were collected from Xishuangbanna Tropical Botanical Garden, Yunnan Province, China, in May, 2017 and authenticated by Professor You-Kai Xu of Xishuangbanna Tropical Botanical Garden, Chinese Academy of Sciences. A voucher specimen has been deposited in School of Pharmaceutical Sciences, Chongqing University (Accession number CRZ2017CBS).

Extraction and Isolation. The air-dried leaves and twigs of *C. bejolghota* (10.0 kg) were powdered and extracted with 95% EtOH (4 × 35 L, 3 days each time) at room temperature. The solvent was concentrated under reduced pressure to obtain a crude extract (1.2 kg), which was suspended in H_2O (2 L) and successively partitioned with petroleum ether (PE, 5 × 2 L), EtOAc (5 × 2 L), and *n*-BuOH (5 × 2 L). The PE and EtOAc extracts were combined together (370 g)

based on the similar TLC profiles and then fractionated by a silica gel column chromatography (CC) eluted with gradient CH_2Cl_2-MeOH (100:1, 50:1, 25:1, 10:1, 5:1, 3:1, 2:1, 1:1, 1:3, each 1 L, v/v) to afford six fractions (A−F). Fractions C (14.8 g), D (19.1 g) and E (38.1 g) were chromatographed on a MCI gel column eluted with MeOH-H_2O (7:3, 8:2, 9:1, 10:0, each 1 L, v/v) to produce subfractions C1−C2, D1−D3, E1−E4, respectively.

Fraction C2 (2.2 g) was separated by a silica gel CC eluted with EtOAc-MeOH (50:1, 30:1, 10:1, each 1 L, v/v) to get Fr.C2a−Fr.C2c. Fr.C2b (136.2 mg) was purified by semi-preparative HPLC (MeCN-H_2O, 5:5, v/v) to yield **13** (8.0 mg, t_R 42.1 min). Fr.C2c (93.0 mg) was separated by a Sephadex LH-20 CC (CH_2Cl_2-MeOH, 1:1, v/v) and then semi-preparative HPLC with MeOH-H_2O (50:50→80:20, v/v) to obtain **16** (8.0 mg, t_R 30.0 min).

Fraction D2 (1.7 g) was separated using a silica gel CC eluted with CH_2Cl_2-MeOH (50:1, 40:1, 30:1, 15:1, 10:1, each 1 L, v/v) to give Fr.D2a−Fr.D2d. Fr.D2b (147.3 mg) was purified by a Sephadex LH-20 CC eluted with CH_2Cl_2-MeOH (1:1, v/v) and then semi-preparative HPLC with MeOH-H_2O (40:60→80:20, v/v) to yield **10** (2.2 mg, t_R 26.8 min), **11** (6.6 mg, t_R 29.3 min), **12** (5.0 mg, t_R 32.9 min) and a mixture (10.0 mg), which was then purified repeatedly by semi-preparative HPLC eluted with MeCN-H_2O (10:90→90:10, v/v) to obtain **9** (6.5 mg, t_R 27.5 min). Fr.D2c (184.1 mg) was separated by a Sephadex LH-20 CC eluted with CH_2Cl_2-MeOH (1:1) to give Fr.D2c1 and Fr.D2c2. Fr.D2c1 (108.2 mg) was purified by semi-preparative HPLC eluted with MeOH-H_2O (40:60→80:20, v/v) to obtain **14** (30.5 mg, t_R 22.8 min) and **15** (19.3 mg, t_R 25.1 min). Similarly, Fr.D2c2 (40.5 mg) produced **7** (3.2 mg, t_R 20.9 min) by semi-preparative HPLC with MeCN-H_2O (30:70, v/v). Fr.D2d (203.5 mg) was purified by a Sephadex LH-20 CC eluted with CH_2Cl_2-MeOH (1:1, v/v) and then semi-preparative HPLC with MeOH-H_2O (40:60→90:10, v/v) to obtain **2** (28.2 mg, t_R 33.1 min) and a mixture, which was then purified by

semi-preparative HPLC eluted with MeCN-H_2O (40:60, v/v) to yield **1** (5.9 mg, t_R 17.3 min), **3** (8.5 mg, t_R 18.3 min) and **4** (7.0 mg, t_R 18.6 min).

Fraction E1 (1.1 g) was partitioned into Fr.E1a−Fr.E1c by a silica gel CC eluted with CH_2Cl_2-MeOH (30:1, 20:1, 10:1, 5:1, each 1 L, v/v). Fr.E1a (172.5 mg) was separated by a Sephadex LH-20 CC (CH_2Cl_2-MeOH, 1:1, v/v) to give two subfractions, which were then purified by semi-preparative HPLC (MeCN-H_2O, 20:80, v/v) to yield **17** (9.0 mg, t_R 21.4 min), **18** (3.0 mg, t_R 26.6 min), **19** (7.0 mg, t_R 29.2 min) and **20** (4.0 mg, t_R 24.7 min), **21** (5.0 mg, t_R 26.6 min), respectively. Fraction E2 (2.6 g) was separated using a silica gel CC eluted with CH_2Cl_2-MeOH (50:1, 40:1, 30:1, 15:1, 10:1, 5:1, each 1 L, v/v) to give Fr.E2a (1080.8 mg) and Fr.E2b (622.0 mg). Fr.E2b (208.1 mg) was purified by a Sephadex LH-20 CC eluted with CH_2Cl_2-MeOH (1:1, v/v) and then semi-preparative HPLC with MeCN-H_2O (25:75→100:0, v/v) to obtain **5** (4.5 mg, t_R 22.3 min) and **6** (4.0 mg, t_R 23.5 min). Fraction E3 (890.0 mg) was separated by a silica gel CC eluted with CH_2Cl_2-MeOH (60:1, 40:1, 30:1, 15:1, 10:1, each 1 L, v/v) to get Fr.E3a−Fr.E3c. Fr.E3b (140.5 mg) was purified by a Sephadex LH-20 CC (CH_2Cl_2-MeOH, 1:1, v/v) and then semi-preparative HPLC (MeOH-H_2O, 10:90→100:0, v/v) to yield **8** (2.3 mg, t_R 38.2 min).

Bejolghotin A (**1**): white solid; $[\alpha]_D^{24}$ −24 (*c* 1.2, MeOH); UV (MeOH) λ_{max} (log ε) 257 (3.32), 228 (3.61), 200 (3.74); CD (MeOH): λ_{max} ($\Delta\varepsilon$) λ_{251} (+3.28), λ_{289} (+3.72), λ_{327} (−4.37); IR (KBr) ν_{max} 3497, 2931, 2311, 1701, 1597, 1512, 1460, 1426, 1328, 1268, 1124, 1032 cm^{-1}; for ^1H and ^{13}C NMR data, see Table 1; HRESIMS *m*/*z* 785.2743 $[M + Na]^+$ (calcd for $C_{41}H_{46}O_{14}Na$, 785.2780).

Bejolghotin B (**2**): white solid; $[\alpha]_D^{27}$ −15 (*c* 4.2, MeOH); UV (MeOH) λ_{max} (log ε) 257 (3.54), 228 (3.83), 198 (3.96); CD (MeOH): λ_{max} ($\Delta\varepsilon$) λ_{223} (+4.00), λ_{263} (+5.08), λ_{326} (−1.57); IR

(KBr) ν_{max} 3501, 2929, 2853, 1701, 1597, 1513, 1460, 1426, 1329, 1270, 1124, 1031 cm^{-1}; for ^{1}H and ^{13}C NMR data, see Table 1; HRESIMS *m/z* 783.2605 $[M + Na]^+$ (calcd for $C_{41}H_{44}O_{14}Na$, 783.2623).

Bejolghotin C (**3**): white solid; $[\alpha]_D^{28}$ −12 (*c* 2.2, MeOH); UV (MeOH) λ_{max} (log ε) 324 (2.60), 280 (2.83), 201 (3.62); CD (MeOH): λ_{max} ($\Delta\varepsilon$) λ_{235} (+1.74), λ_{264} (−0.29), λ_{294} (+2.11), λ_{330} (−2.69); IR (KBr) ν_{max} 3507, 2929, 2856, 1709, 1596, 1512, 1460, 1372, 1330, 1269, 1124, 1031 cm^{-1}; for ^{1}H and ^{13}C NMR data, see Table 1; HRESIMS *m/z* 783.2598 $[M + Na]^+$ (calcd for $C_{41}H_{44}O_{14}Na$, 783.2623).

Bejolghotin D (**4**): white solid; $[\alpha]_D^{28}$ −24 (*c* 1.2, MeOH); UV (MeOH) λ_{max} (log ε) 257 (3.36), 228 (3.65), 199 (3.78); CD (MeOH): λ_{max} ($\Delta\varepsilon$) λ_{237} (+3.70), λ_{269} (−2.50), λ_{300} (+2.09), λ_{330} (−1.83); IR (KBr) ν_{max} 3483, 2928, 2856, 1708, 1596, 1512, 1460, 1372, 1329, 1269, 1123, 1030 cm^{-1}; for ^{1}H and ^{13}C NMR data, see Table 1; HRESIMS *m/z* 783.2615 $[M + Na]^+$ (calcd for $C_{41}H_{44}O_{14}Na$, 783.2623).

Bejolghotin E (**9**): white solid; $[\alpha]_D^{24}$ −14 (*c* 2.4, MeOH); UV (MeOH) λ_{max} (log ε) 327 (1.24), 285 (1.24), 199 (2.37); CD (MeOH): λ_{max} ($\Delta\varepsilon$) λ_{257} (+4.32), λ_{295} (+2.83), λ_{345} (−2.46); IR (KBr) ν_{max} 3499, 3057, 2930, 2855, 1706, 1596, 1514, 1460, 1372, 1328, 1267, 1159, 1123, 1032 cm^{-1}; for ^{1}H and ^{13}C NMR data, see Table 2; HRESIMS *m/z* 785.2752 $[M + Na]^+$ (calcd for $C_{41}H_{46}O_{14}Na$, 785.2780).

Bejolghotin F (**10**): white solid; $[\alpha]_D^{25}$ −40 (*c* 0.7, MeOH); UV (MeOH) λ_{max} (log ε) 329 (1.15), 283 (1.10), 203 (2.14); CD (MeOH): λ_{max} ($\Delta\varepsilon$) λ_{237} (+3.79), λ_{266} (−1.78), λ_{339} (−3.38); IR (KBr) ν_{max} 3363, 2928, 2856, 1705, 1607, 1516, 1461, 1375, 1322, 1262, 1214, 1160, 1108, 1033 cm^{-1}; for ^{1}H and ^{13}C NMR data, see Table 2; HRESIMS *m/z* 635.2093 $[M + Na]^+$ (calcd for $C_{32}H_{36}O_{12}Na$, 635.2099).

Bejolghotin G (**11**): white solid; $[\alpha]_D^{26}$ –60 (*c* 0.15, MeOH); UV (MeOH) λ_{max} (log ε) 326 (4.38), 285 (4.24), 206 (5.09); CD (MeOH): λ_{max} ($\Delta\varepsilon$) λ_{230} (+2.71), λ_{260} (−0.88), λ_{338} (−2.21); IR (KBr) ν_{max} 3425, 2930, 2852, 1700, 1604, 1515, 1460, 1428, 1370, 1319, 1271, 1243, 1215, 1175, 1115, 1058, 1032 cm^{-1}; for ^1H and ^{13}C NMR data, see Table 2; HRESIMS *m*/*z* 619.2160 [M + Na]$^+$ (calcd for $C_{32}H_{36}O_{11}Na$, 619.2150).

Antioxidant Assay. The antioxidant activity was performed by evaluating the ability to scavenge the DPPH radical according to previous publication.[5,27] All the test samples (the isolates and positive controls, L-ascorbic acid and BHT) were dissolve in EtOH to get stock solutions (1 mM). Various concentrations of test samples (20 μL), which were prepared by series dilution of the stock solutions, were added to 150 μM DPPH in EtOH (180 μL). The mixture was shaken and then incubated for 30 min in darkness at 37 °C. The absorbance was read at 517 nm and each sample was tested in triplicate.

Human Cancer Cell Proliferation Inhibitory Assay. The isolates and positive control (adriamycin) were assayed for growth inhibition using HCT-116 (colon carcinoma), A549 (lung), and MDA-MB-231 (breast) human cancer cell lines and BEAS-2B (bronchial epithelial) and L02 (liver) human normal cell lines as per published method.[28] The samples were dissolved in DMSO (10 mM) and further diluted with DMEM medium to obtain stock solutions with the final desired concentration. Eight different concentrations of test samples (100 μL), which were prepared by series dilution of the stock solutions, were added to each well containing the test cancer cell line (100 μL). After incubation under 5% CO_2 for 48 h, an aliquot (25 μL) of MTT solution (1 mg/mL) was added to each well, and the plates were incubated for another 3 h. After removing the medium, DMSO (200 μL) was added to each well and then the plates were shaken.

Optical density was measured at 570 nm and each sample was tested in triplicate to calculate the IC_{50} values.

RESULTS AND DISCUSSION

Purification and structural elucidation afforded 21 pure isolates (Figure 1), including 7 new (**1**−**4** and **9**−**11**) and 14 known (**5**−**8** and **12**−**21**) compounds, which were then classified as 9 lignans (**9**−**17**) and 12 neolignans (**1**−**8** and **18**−**21**). On the other hand, all the isolates could be further categorized as lignans (**11**−**13** and **17**), sesquilignans (**9**, **10** and **16**), dilignans (**14** and **15**), neolignans (**7**, **8**, **18**−**21**) and sesquineolignans (**1**−**6**). New compounds were elucidated by extensive spectroscopic data and electronic circular dichroism analyses, while known compounds were identified by comparing their spectroscopic data with literatures. All the isolates were evaluated for *in vitro* antioxidant activity by DPPH assay and human cancer cell proliferation inhibition by MTT method, respectively.

Compound **1** possessed a molecular formula $C_{41}H_{46}O_{14}$ according to HRESIMS *m*/*z* 785.2743 $[M + Na]^+$ (calcd for $C_{41}H_{46}O_{14}Na$, 785.2780), corresponding to 19 degrees of unsaturation (DOUs). The IR spectrum indicated the presence of hydroxy (3497 cm^{-1}), carbonyl (1706 cm^{-1}) and aromatic (1597, 1512 and 1460 cm^{-1}) groups. The ^1H and ^{13}C NMR (Table 1) together with HSQC spectrum showed the presence of an ester carbonyl (δ_C 167.1, C-9‴), one set of *trans*-configurated double bond [δ_H 7.50 (dd, J = 15.9 Hz), δ_C 144.8, CH-7‴; δ_H 6.23 (d, J = 15.9 Hz), δ_C 115.7, CH-8‴], four aromatic units including two 1,3,4-trisubstituted [δ_H 7.00 (s, H-2‴), 6.90 (d, J = 8.1 Hz, H-5‴) and 7.02 (d, J = 8.1 Hz, H-6‴); δ_H 6.99 (d, J = 1.8 Hz, H-2″), 6.91 (dd, J = 8.1, 1.8 Hz, H-5″) and 6.77 (d, J = 8.1 Hz, H-6″)] and two 1,3,4,5-tetrasubstituted [δ_H 6.69 (3H, s, H-2, 6); δ_H 6.67 (s, H-2′) and 6.69 (s, H-6′)], five methoxy groups, three oxygenated methines [δ_H 5.58 (d, J = 7.3 Hz), δ_C 87.9, CH-7; δ_H 4.87 (brs), δ_C 71.7, CH-7″; δ_H

4.55 (m), δ_C 83.4, CH-8″], three oxygenated methylenes [δ_H 4.45 (dd, J = 11.9, 7.6 Hz) and 4.33 (dd, J = 11.9, 3.6 Hz), δ_C 62.6, CH_2-9″; δ_H 3.98 (dd, J = 11.0, 6.0 Hz) and 3.93 (dd, J = 11.0, 4.7 Hz), δ_C 64.1, CH_2-9; δ_H 3.70 (2H, t, J = 6.2 Hz), δ_C 62.4, CH_2-9′], one methine [δ_H 3.62 (brd, J = 5.4 Hz), δ_C 54.0, CH-8] and two methylenes [δ_H 2.68 (2H, t, J = 7.6 Hz), δ_C 32.2, CH_2-7′; δ_H 1.89 (2H, t, J = 6.9 Hz), δ_C 34.8, CH_2-8′]. Three proton resonances at δ_H 5.87 (s), 5.54 (s) and 4.21 (d, J = 7.9 Hz) showing no correlations with any carbon signals in the HSQC spectrum were attributable to the hydroxy groups. The structure of **1** was confirmed by detailed analysis of the 2D NMR data (Figure 2A). The fragments of the above-mentioned sp^3 methines and methylenes were established as shown in Figure 2A by the ^1H–^1H COSY correlations of H-7/H-8, H-8/H_2-9, H_2-7′/H_2-8′, H_2-8′/H_2-9′, H-7″/H-8″, H-8″/H_2-9″. The HMBC correlations of H-7/C-1 (δ 137.9), C-2 (δ 103.3), C-6 (δ 103.3), C-3′ (δ 127.5) and C-4′ (δ 146.7), H-8/C-1, C-2′ (δ 116.0), C-3′ and C-4′, H_2-9/C-3′, H_2-7′/C-1′ (δ 135.9), C-2′ and C-6′ (δ 112.6), and H_2-8′/C-1′ indicated **1** possessed a dihydrobenzofuran neolignan skeleton. Three methoxy groups to C-3 (δ 153.7), C-5 (δ 153.7) and C-5′ (δ 144.4) were accomplished by the HMBC correlations from 3-OMe (δ 3.83, s), 5-OMe (δ 3.83, s) and 5′-OMe (δ 3.89, s) to the corresponding carbon signals. The fragment of H-7″–H-8″–H_2-9″ was connected to one 1,3,4-trisubstituted aromatic unit, which was accomplished by the HMBC correlations from 4″-OH (δ 5.54, s) to C-3″ (δ 146.6), C-4″ (δ 144.9) and C-5″ (δ 114.3), and from 3″-OMe (δ 3.89, s) to C-3″, to form a phenylpropyl moiety by the HMBC correlations of H-7″/C-1″ (δ 130.8) and C-6″ (δ 119.0), H-2″ and H-6″/C-7″. Furthermore, one hydroxy group was linked to C-7″ based on the HMBC correlations of 7″-OH (δ 4.21)/C-1″ and C-7″. One feruloyl unit was elucidated by the ^1H–^1H COSY correlations of H-7‴/H-8‴ and HMBC correlations of H-7‴/C-1‴ (δ 127.2), C-2‴ (δ 109.4), C-6‴ (δ 123.2) and C-9‴, H-8‴/C-1‴ and C-9‴, 4‴-OH/ C-3‴ (δ 146.9), C-4‴ (δ 148.1) and C-5‴ (δ 114.8), and 3‴-OMe (δ 3.92, s)

to C-3‴, which was then connected to C-9″ through the ester bond by the HMBC correlation of H_2-9″/C-9‴ to form a dihydroconiferyl ferulate unit.[29,30] Although there is no direct HMBC cross peak from H-8″ to C-4 observed, the chemical shift of C-4 (δ 134.4) supported the linkage of C-4 to C-8″ through the ether bond to connect these two dihydrobenzofuran neolignan and dihydroconiferyl ferulate units, but not C-4 to –OH (ca. δ 146.0).[31] Lastly, the other two hydroxyl groups were attached to C-9 and C-9′ to satisfy the molecular formula even there were no any useful HMBC correlations observed. Therefore, the planar structure of **1** was established. The relative configuration of **1** was determined by the ROESY experiment (Figure 2A) and interpretation of chemical shifts and ^{1}H–^{1}H coupling constants. For dihydrobenzofuran neolignan unit, the *trans*-relationship between H-7 and H-8 was implied by the coupling constant of 7.3 Hz between them, which was further supported by the ROESY correlations of H-7/H_2-9. For the dihydroconiferyl ferulate unit, the *erythro* configuration of H-7″ and H-8″ was confirmed by the small coupling constant (H-7″ appeared as a slightly broad singlet) between them and almost the same chemical shifts of CH-7″ and CH-8″ as (−)-7′*R*,8′*S*-*erythro*-carolignan Z[29] and *erythro*-carolignan F.[30] The absolute configuration of **1** was elucidated by electronic circular dichroism (ECD) analysis. Among the four possible configuration **1a** (7*S*,8*R*,7″*R*,8″*S*), **1a′** (7*R*,8*S*,7″*S*,8″*R*), **1b** (7*S*,8*R*,7″*S*,8″*R*) and **1b′** (7*R*,8*S*,7″*R*,8″*S*), the theoretical ECD spectra of **1a** and **1b** were calculated using the time-dependent density functional theory (TDDFT) at the B3LYP/6-311++G(2d,p) level in the Conductor-like Polarizable Continuum Model (CPCM),[32-34] and the results showed that the experimental ECD spectrum of **1** matched well with the calculated ECD spectrum of **1a** (Figure 3A), which assigned the absolute configuration of **1** as (7*S*,8*R*,7″*R*,8″*S*). Thus, **1** was identified as shown and named as bejolghotin A.

Compound **2** was assigned the molecular formula $C_{41}H_{44}O_{14}$ by HRESIMS *m*/*z* 783.2605 [M + Na]$^+$ (calcd for $C_{41}H_{44}O_{14}Na$, 783.2623) with 2 mass unit less than that of **1**. Direct comparison of the NMR data (Table 1) of **2** with **1** also displayed their only differences as the presence of one additional *trans*-configurated double bond [δ_H 6.55 (d, J = 15.8 Hz), δ_C 131.3, CH-7′; δ_H 6.24 (m), δ_C 126.8, CH-8′] at **2** and the absences of two sp^3 methylenes at **1**, which resulted in that the chemical shift of CH_2-9′ down-field shifted *ca.* $\Delta\delta$ 0.5 ppm as compared with that of **1**. The planar structure of **2** was further confirmed by the analysis of ^{1}H–^{1}H COSY, HSQC and HMBC spectral data (Supporting Information, Figure S1). Similarly, the coupling constant ($J_{7,8}$ = 6.9 Hz) and the ROESY cross peaks between H-7 and H_2-9 indicated the *trans*-configuration of H-7 and H-8. H-7″ appearing as a slightly broad singlet and the identical chemical shifts of CH-7″ and CH-8″ with **1** also confirmed the *erythro* configuration of H-7″ and H-8″ at **2**. The experimental ECD spectrum of **2** matched well with the calculated ECD spectrum of **2b** (7*S*,8*R*,7″*S*,8″*R*) other than **2a** (7*S*,8*R*,7″*R*,8″*S*), **2a**′ (7*R*,8*S*,7″*S*,8″*R*) and **2b**′ (7*R*,8*S*,7″*R*,8″*S*) (Figure 3B), suggesting the absolute configuration of **2** as (7*S*,8*R*,7″*S*,8″*R*). Therefore, **2** was elucidated and named as bejolghotin B.

Compound **3** had the same molecular formula $C_{41}H_{44}O_{14}$ as **2** by HRESIMS data. Furthermore, compounds **3** and **2** also had very similar NMR data except for the slight discrepancy arising from the oxygenated methines (CH-7″ and CH-8″) and methylene (CH_2-9″). The comprehensive analyses of 1D and 2D NMR spectral data (Supporting Information, Figure S2) revealed **3** with the same planar structure as **2**, suggesting that **3** was a *threo* diastereoisomer of **2**, which was further confirmed by the coupling constant between H-7″ and H-8″ (8.0 Hz) and the identical chemical shifts of CH-7″ and CH-8″ of *threo*-carolignan E[29,30] and *threo*-carolignan K.[30] As for four possible configurations **3a** (7*S*,8*R*,7″*R*,8″*R*), **3a**′ (7*R*,8*S*,7″*S*,8″*S*), **3b**

(7*S*,8*R*,7″*S*,8″*S*) and **3b**′ (7*R*,8*S*,7″*R*,8″*R*), the experimental ECD spectrum of **3** matched well with the calculated ECD spectrum of **3a** (Figure. 3C), assigning the absolute configuration of **3** as 7*S*,8*R*,7″*R*,8″*R*. Thus, **3** was determined and named as bejolghotin C.

Compound **4** also had the same molecular formula $C_{41}H_{46}O_{14}$ as **2**. The NMR data (Table 1) of **4** was identical to those of **2**, and the only difference was that one set of *cis*-configurated double bond [δ_H 6.74 (d, J = 12.8 Hz), δ_C 144.0, CH-7‴; δ_H 5.74 (d, J = 12.8 Hz), δ_C 116.6, CH-8‴] at **4** replaced the corresponding *trans*-configurated double bond at **2**, which was assigned by the HMBC correlations of H-7‴ and H-8‴/ C-9‴ (δ_C 166.3). The planar structure of **4** was further confirmed by the detailed analysis of 2D NMR data (Supporting Information, Figure S3). Similarly, the *trans*-configuration of H-7 and H-8 was determined by the coupling constant ($J_{7,8}$ = 6.3 Hz) and the ROESY correlation of H-7/H_2-9, and the *erythro* configuration of H-7″ and H-8″ was determined by the small coupling constant (H-7″ displayed as a slightly broad singlet) and the identical chemical shifts of CH-7″ and CH-8″ with **1** and **2**. Similar as **2**, the experimental ECD spectrum of **4** matched with the calculated ECD spectrum of **4a** (7*S*,8*R*,7″*S*,8″*R*) other than **4a**′ (7*R*,8*S*,7″*R*,8″*S*), **4b** (7*S*,8*R*,7″*R*,8″*S*) and **4b**′ (7*R*,8*S*,7″*S*,8″*R*) (Figure 3D), suggesting the absolute configuration of **4** as (7*S*,8*R*,7″*S*,8″*R*). Therefore, **4** was confirmed and named as bejolghotin D.

The molecular formula of **9** was assigned as $C_{41}H_{46}O_{14}$ based on HRESIMS *m*/*z* 785.2752 $[M + Na]^+$ (calcd for $C_{41}H_{46}O_{14}Na$, 785.2780), corresponding to 19 DOUs. IR spectrum showed the absorption bands for OH (3499 cm^{-1}), carbonyl (1706 cm^{-1}) and aromatic (1596, 1514 and 1460 cm^{-1}) functionalities. The ^1H and ^{13}C NMR with the help of HSQC spectrum (Table 2) also revealed the presence of an ester carbonyl (δ_C 167.2, C-9‴), one set of *trans*-configurated double bond [δ_H 7.51 (dd, J = 15.9 Hz), δ_C 144.8, CH-7‴; δ_H 6.24 (d, J = 15.9 Hz), δ_C 115.7, CH-8‴],

two 1,3,4-trisubstituted aromatic units [δ_H 7.01 (s, H-2‴), 6.90 (d, J = 8.1 Hz, H-5‴) and 7.03 (d, J = 8.1 Hz, H-6‴); δ_H 7.02 (s, H-2″), 6.87 (d, J = 8.1 Hz, H-5″) and 6.77 (d, J = 8.1 Hz, H-6″)], two methoxy groups, two oxygenated methines [δ_H 4.89 (brs), δ_C 71.7, CH-7″; δ_H 4.56 (m), δ_C 83.3, CH-8″], one oxygenated methylene [δ_H 4.46 (dd, J = 11.8, 7.5 Hz) and 4.32 (dd, J = 11.8, 3.7 Hz), δ_C 62.6, CH_2-9″], and three hydroxy groups [δ_H 5.87 (s), 4‴-OH; 5.55 (s), 4″-OH; 4.26 (d, J = 9.8 Hz), 7″-OH], which was assignable as a dihydroconiferyl ferulate unit and confirmed by the detailed analysis of the ^{1}H–^{1}H COSY and HMBC correlations (Figure 2B). Moreover, one fragment including one oxygenated sp^3 methine [δ_H 4.85 (d, J = 5.9 Hz), δ_C 83.1, CH-7′], two oxygenated sp^3 methylenes [δ_H 4.07 (brt, J = 7.6 Hz) and 3.76 (dd, J = 8.1, 7.2 Hz), δ_C 73.3, CH_2-9; δ_H 3.93 (m) and 3.80 (m), δ_C 61.1, CH_2-9′], two sp^3 methines [δ_H 2.72 (m), δ_C 42.6, CH-8; δ_H 2.41 (brt, J = 6.6 Hz), δ_C 52.6, CH-8′] and one sp^3 methylene [δ_H 2.90 (dd, J = 13.5, 5.2 Hz) and 2.56 (dd, J = 13.5, 10.7 Hz), δ_C 33.4, CH_2-7] was confirmed by the ^{1}H–^{1}H COSY correlations of H_2-7/H-8, H-8/H_2-9, H-7′/H-8′, H-8′/H_2-9′ and H-8/H-8′, and then C-9 and C-7′ were connected through the ether bond by the HMBC correlations of H-7′/C-9 and H_2-9/C-7′. One additional 1,3,4-trisubstituted aromatic unit was linked with C-7 by the HMBC correlations of H_2-7/C-1 (δ 132.3), C-2 (δ 111.3) and C-6 (δ 121.3), H-2 [δ 6.68 (s)] and H-6 [δ 6.69 (d, J = 8.2 Hz)]/C-7, 3-OMe [δ 3.86 (s)]/C-3 (δ 146.7), and 4-OH [δ 5.51 (s)]/C-3, C-4 (δ 144.2) and C-5 (δ 114.6). One 1,3,4,5-tetrasubstituted aromatic unit was connected to C-7′ by the HMBC correlations of H-7′/C-1′ (δ 139.8), C-2′ (δ 102.8) and C-6′ (δ 102.8), H-2′ [δ 6.60 (s)] and H-6′ [δ 6.60 (s)]/C-7′, 3′-OMe [δ 3.85 (s)]/C-3′ (δ 153.6), and 5′-OMe [δ 3.85 (s)]/C-5′ (δ 153.6). The above-mentioned data suggested a 2-aryl-4-benzyltetrahydrofuranoid lignan skeleton. Although there is no direct HMBC cross peak from H-8″ to C-4 observed, these two 2-aryl-4-benzyltetrahydrofuranoid lignan and dihydroconiferyl ferulate units were connected through C-4′–O–C-8″ by the ROESY

correlations of H-7″ and H-8″/3′-OMe or 5′-OMe. Thus, the planar structure of **9** was determined. As for the relative configuration of **9**, the *erythro* configuration of H-7″ and H-8″ in the dihydroconiferyl ferulate unit was still confirmed by the small coupling constant (H-7″ appeared as a slightly broad singlet) between them and the identical chemical shifts of CH-7″ and CH-8″ with **1**, **2**, (−)-7′*R*,8′*S*-*erythro*-carolignan Z[29] and *erythro*-carolignan F[30]. The 8,8′-*cis* and 7′,8′-*trans* configuration in the 2-aryl-4-benzyltetrahydrofuranoid lignan unit were determined by the ROESY correlations of H-7′/H-7b, H-7′/H_2-9′, and H_2-7/H_2-9′. Similarly, the absolute configuration of **9** was elucidated as (8*S*,7′*R*,8′*S*,7″*S*,8″*R*) by ECD analysis, while the experimental ECD spectrum of **9** matched with the calculated ECD spectrum of **9a** (8*S*,7′*R*,8′*S*,7″*S*,8″*R*) other than **9a′** (8*R*,7′*S*,8′*R*,7″*R*,8″*S*), **9b** (8*S*,7′*R*,8′*S*,7″*R*,8″*S*) and **9b′** (8*R*,7′*S*,8′*R*,7″*S*,8″*R*). Therefore, the structure of **9** was elucidated and named as bejolghotin E.

Compound **10** possessed the molecular formula $C_{32}H_{36}O_{12}$ based on the HRESIMS *m*/*z* 635.2093 $[M + Na]^+$ (calcd for $C_{32}H_{36}O_{12}Na$, 635.2099), corresponding to 15 DOUs. The ^1H, ^{13}C NMR and HSQC spectrum (Table 2) revealed the presence of a (*E*)-feruloyl moiety: an ester carbonyl (δ_C 167.1, C-9″), one set of *trans*-configurated double bond [δ_H 7.47 (dd, *J* = 15.9 Hz), δ_C 145.6, CH-7″; δ_H 6.19 (d, *J* = 15.9 Hz), δ_C 114.9, CH-8″], one 1,3,4-trisubstituted aromatic units [δ_H 6.98 (d, *J* = 1.5 Hz, H-2″), 6.92 (d, *J* = 8.2 Hz, H-5″) and 7.04 (dd, *J* = 8.2, 1.5 Hz, H-6″)], one methoxy group [δ_H 3.95 (s), δ_C 56.2, 3″-OMe], and one hydroxyl group [δ_H 5.88 (s), 4″-OH], which was confirmed by the detailed analysis of the ^1H–^1H COSY and HMBC correlations (Supporting Information, Figure S4). In addition, one fragment including two oxygenated sp^3 methines [δ_H 4.92 (d, *J* = 5.9 Hz), δ_C 73.0, CH-7; δ_H 4.91 (d, *J* = 6.3 Hz), δ_C 84.4, CH-7′], two oxygenated sp^3 methylenes [δ_H 4.23 (brt, *J* = 7.8 Hz) and 4.16 (dd, *J* = 8.8, 7.5 Hz), δ_C 69.6, CH_2-9; δ_H 4.60 (dd, *J* = 11.3, 5.9 Hz) and 4.37 (dd, *J* = 11.3, 7.7 Hz), δ_C 63.0, CH_2-9′], two sp^3

methines [δ_H 2.88 (m), δ_C 47.5, CH-8; δ_H 2.53 (m), δ_C 48.7, CH-8′] was constructed by the $^1H–^1H$ COSY correlations of H-7/H-8, H-8/H_2-9, H-7′/H-8′, H-8′/H_2-9′ and H-8/H-8′, and then C-9 and C-7′ were connected through the ether bond by the HMBC correlations of H_2-9/C-7′. Two 1,3,4,5-tetrasubstituted aromatic units were linked with C-7 and C-7′ by the HMBC correlations of H-7/C-1 (δ 134.6), C-2 (δ 102.9) and C-6 (δ 102.9), H-2 and H-6 [both δ 6.60 (s)]/C-7, 3-OMe [δ 3.88 (s)]/C-3 (δ 147.4), 5-OMe [δ 3.88 (s)]/C-5 (δ 147.4), 4-OH [δ 5.44 (s)]/C-3 and C-5, and H-7′/C-1′ (δ 134.5), C-2′ (δ 102.8) and C-6′ (δ 102.8), H-2′ and H-6′ [both δ 6.59 (s)]/C-7′, 3′-OMe [δ 3.87 (s)]/C-3′ (δ 147.2), 5′-OMe [δ 3.87 (s)]/C-5′ (δ 147.2), and 4′-OH [δ 5.49 (s)]/C-3 and C-5, respectively. The above-mentioned data suggested a 2-aryl-4-benzyltetrahydrofuranoid lignan skeleton with one substituted –OH located at C-7. The (*E*)-feruloyl moiety was connected to 9′ by the HMBC correlations of H_2-9′/C-9″ and the chemical shifts of CH_2-9′. Similar to **9**, the ROESY correlations of H-7′/H_2-9′ confirmed the 7′,8′-*trans* configuration, and then the 8,8′-*cis* configuration could be assigned by the similar coupling constants of H_2-9 as that of **9**. Despite of the configuration of C-7, which was not determined in this study and will be further studied in the future, the experimental ECD spectrum of **10** match with the calculated ECD spectrum of **10a′** (Figure. 3F) amongst the two possible configurations **10a** (8*R*,7′*S*,8′*R*) and **10a′** (8*S*,7′*R*,8′*S*), suggesting the (8*S*,7′*R*,8′*S*) absolute configuration of **10**. Therefore, compound **10** was elucidated named as bejolghotin F.

Compound **11** was assigned the molecular formula $C_{32}H_{36}O_{11}$ by HRESIMS *m*/*z* 619.2160 $[M + Na]^+$ (calcd for $C_{32}H_{36}O_{11}Na$, 619.2150), corresponding to 15 DOUs. Similarly, the NMR spectrum (Table 2) also revealed the presence of a (*E*)-feruloyl moiety: an ester carbonyl (δ_C 167.5, C-9″), one set of *trans*-configurated double bond [δ_H 7.59 (dd, J = 16.0 Hz), δ_C 145.6, CH-7″; δ_H 6.29 (d, J = 16.0 Hz), δ_C 115.3, CH-8″], one 1,3,4-trisubstituted aromatic units [δ_H 7.02 (s,

H-2″), 6.91 (d, J = 8.1 Hz, H-5″) and 7.05 (d, J = 8.1 Hz, H-6″)], one methoxy group [δ_H 3.93 (s), δ_C 56.3, 3″-OMe] and one hydroxyl group [δ_H 5.80 (s), 4″-OH]. Besides, one fragment including three sp^3 methines [δ_H 4.27 (d, J = 6.3 Hz), δ_C 42.5, CH-7′; δ_H 2.24 (m), δ_C 44.7, CH-8′; δ_H 1.85 (m), δ_C 39.3, CH-8], two oxygenated sp^3 methylenes [δ_H 4.30 (dd, J = 11.4, 3.8 Hz) and 4.17 (dd, J = 11.4, 5.1 Hz), δ_C 65.2, CH_2-9′; δ_H 3.73 (dd, J = 10.4, 3.6 Hz) and 3.67 (dd, J = 10.4, 5.9 Hz), δ_C 65.9, CH_2-9], one sp^3 methylene [δ_H 2.74 (m, 2H), δ_C 32.8, CH_2-7] was constructed by the ^1H–^1H COSY correlations of H_2-7/H-8, H-8/H_2-9, H-7′/H-8′, H-8′/H_2-9′ and H-8/H-8′, suggesting an aryltetralin lignan skeleton, which was further confirmed by the detailed analysis of the HMBC correlations (Figure 2C). One 1,3,4,5-tetrasubstituted aromatic unit was connected to C-7′ by the HMBC correlations of H-7′/C-1′ (δ 137.8), C-2′ (δ 105.2) and C-6′ (δ 105.2), H-8′/C-1′, H-2′ and H-6′ [both δ 6.34 (s)]/C-7′, 3′-OMe [δ 3.78 (s)]/C-3′ (δ 147.0), 5′-OMe [δ 3.78 (s)]/C-5′ (δ 147.0), 4′-OH [δ 5.36 (s)]/C-3′, C-4′ (δ 133.1) and C-5′. Another aromatic unit was assigned with the connection of C-1/C-7 and C-6/C-7′ by the HMBC correlations of H-7′/C-1 (δ 128.8), C-5 (δ 145.6) and C-6 (δ 124.8), H-8′/C-6, H_2-7/C-1, C-2 (δ 106.1) and C-6 (δ 124.8), H-8/C-1, 3-OMe [δ 3.98 (s)]/C-3 (δ 146.4), 5-OMe [δ 3.36 (s)]/C-5, and 4-OH [δ 5.36 (s)]/C-3, C-4 and C-5. The (*E*)-feruloyl moiety was connected to 9′ by the HMBC correlations of H_2-9′/C-9″ and the chemical shifts of CH_2-9′. Then the planar structure of **11** was determined with the similar structure of **12** and **13**,[35] which were discovered in this study too. The 7′,8′-*trans* and 8′,8-*trans* configurations were assigned by comparing the chemical shifts and coupling constants of corresponding protons of **11** with **12** and **13**, and further supported by the ROESY correlations of H-8/H_2-9′ and H-8′/H-2′ or H-6′. Interestingly, the absolute configuration of **11** was elucidated as (8*S*,7′*R*,8′*S*), which was different with **12** and **13**, by electronic circular dichroism analysis, while the experimental ECD spectrum of **11** matched with the calculated ECD spectrum of **11a′**

amongst the two possible configurations **11a** (8*R*,7′*S*,8′*R*) and **11a**′ (8*S*,7′*R*,8′*S*). Thus, compound **11** was elucidated and named as bejolghotin G.

Known compounds were identified as (7′*R*,8′*S*)-7-(4-hydroxy-3-methoxyphenyl)-8-(4-(2,6-dimethoxyphenyl)-5-(3-(*E*)-hydroxyprop-1-enyl)-7-methoxybenzofuran-2-yl)-2-methoxyphenoxy) propane-7,9-diol (**5**),[36] (7′*S*,8′*S*)-7-(4-hydroxy-3-methoxyphenyl)-8-(4-(2,6-dimethoxyphenyl)-5-(3-(*E*)-hydroxyprop-1-enyl)-7-methoxybenzofuran-2-yl)-2-methoxyphenoxy) propane-7,9-diol (**6**),[36] 7*S*,8*R*-dihydrodehydrodiconiferyl alcohol (**7**),[37] (2*S*,3*R*)-dehydrodiconiferyl alcohol (**8**),[38] (7′*S*,8′*R*,8*R*)-lyoniresinol-9-*O*-(*E*)-feruloyl ester (**12**),[35] (7′*S*,8′*R*,8*R*)-lyoniresinol-9,9′-di-*O*-(*E*)-feruloyl ester (**13**),[35] (+)-7*R*,7′*R*,7″*R*,7‴*S*,8*S*,8′*S*,8″*S*,8‴*S*)-4″,4‴-dihydroxy-3,3′,3″,3‴,5,5′-hexamethoxy-7,9′;7′,9-diepoxy-4,8″;4′,8‴-bisoxy-8,8′-dineolignan-7″,7‴,9″,9‴-tetraol (**14**),[39] (+)-7*R*,7′*R*,7″*S*,7‴*S*,8*S*,8′*S*,8″*S*,8‴*S*)-4″,4‴-dihydroxy-3,3′,3″,3‴,5,5′-hexamethoxy-7,9′;7′,9-diepoxy-4,8″;4′,8‴-bisoxy-8,8′-dineolignan-7″,7‴,9″,9‴-tetraol (**15**),[39] (−)-(7*R*,7′*R*,7″*R*,8*S*,8′*S*,8″*S*)-4′,4″-dihydroxy-3,3′,3″,5-tetramethoxy-7,9′:7′,9-diepoxy-4,8″-oxy-8,8′-sesquineolignan-7″,9″-diol (**16**),[40] icariol A2 (**17**),[41] (7*S*,8*R*)-*erythro*-guaiacylglycerol-*β*-*O*-4′-dihydroconiferyl ether (**18**),[42] (7*R*,8*R*)-*threo*-guaiacyl-glycerol-*β*-*O*-4′-dihydroconiferyl ether (**19**),[42] (7*S*,8*R*)-1-(4-hydroxy-3-methoxyphenyl)-2-{4-[(*E*)-3-hydroxy-1-propenyl]-2-methoxyphe-noxy}-1,3-propanediol (**20**),[43,44] and (7*R*,8*R*)-1-(4-hydroxy-3-methoxyphenyl)-2-{4-[(*E*)-3-hydroxy-1-propenyl]-2-methoxyphe-noxy}-1,3-propanediol (**21**)[44] by comparing their NMR, ESIMS, ORD and ECD data with the literatures. All of the known compounds were isolated from *C. bejolghota* for the first time.

Due to the well-known antioxidant activity of lignans and neolignans, all the isolates were evaluated for antioxidant activity using DPPH assay.[27] The tested compounds except for **16** exhibited good inhibition against the DPPH radical comparable to positive control L-ascorbic

acid and BHT, as shown in Table 3. Amongst, new compounds **1**–**4**, **9**–**11** and known compounds **5**, **6**, **12**–**14** were the first time to report their DPPH radical-scavenging activity while the other known compounds have been reported before and our results were consistent with the previous report.[37,41–43,45,46]

All the isolates were also evaluated *in vitro* for the human cancer cell proliferation inhibition by using HCT-116 (colon carcinoma), A549 (lung) and MDA-MB-231 (breast) human cancer cell lines and BEAS-2B (bronchial epithelial), L02 (liver) human normal cell lines with the MTT method.[28] Firstly, all the isolates were tested at 10 μM and the results displayed compounds **11**–**13** with strong inhibition around 100% and **1**–**3** with moderate inhibition around 30–50% against cancer cell lines but no inhibition on normal cell lines. Therefore, they were selected for the further evaluation to obtain the IC_{50} values (Table 4). Amongst, compounds **11**–**13** (IC_{50} = 0.78–2.93 μM) especially **13** (IC_{50} = 0.78–0.86 μM) showed strongest activity against all three cancer cell lines comparable to positive control Adriamycin (IC_{50} = 0.29–0.38 μM).

In conclusion, this is the first report for isolating the chemical constituents from *C. bejolghota*, and 21 lignans and neolignans, including 4 new neolignans (**1**–**4**) and 3 new lignans (**9**–**11**), were discovered and characterized, which proved *C. bejolghota* as a rich resource for lignans and neolignans. Amongst the isolates, 20 ones showed comparable antioxidant activity to the positive controls in addition to 3 compounds (**11**–**13**) with strong and the other 3 ones (**1**–**3**) with moderate cancer cell proliferation inhibitory activities. The antioxidant and cancer cell proliferation inhibitory activities for *C. bejolghota* and its constituents were studied for the first time, and the results presented herein confirmed its health benefits as functional food.

ASSOCIATED CONTENT

Supporting Information

The Supporting Information is available free of charge on the ACS Publications website.

Full spectroscopic data (NMR, MS, IR) of new compounds (PDF)

AUTHOR INFORMATION

Corresponding author

*E-mail: crzhang@cqu.edu.cn.

ORCID

Chuan-Rui Zhang: 0000-0002-0376-0369

ABBREVIATIONS USED

BHT, butylatedhydroxytoluene; CC, column chromatography; DMSO, dimethylsulfoxide; DPPH, diphenylpicrylhydrazyl; GC, gas chromatography; HPLC, High-performance liquid chromatography; IR, Infrared; MS, mass Spectrometry; MTT, 3-(4,5-dimethylthiazole-2-yl)-2,5-diphenyltetrazolium bromide; NMR, nuclear magnetic resonance; ORD, optical rotatory dispersion; TLC, thin-layer chromatography; UV, ultraviolet.

ACKNOWLEDGEMENTS

This work was supported by the Open Project of State Key Laboratory of Natural Medicines (No. SKLNMKF202011), Fundamental Research Funds for the Central Universities in China (Project No. 2018CDQYYX0041 and 2019CDQYYX018) and Venture & Innovation Support Program for Chongqing Overseas Returnees (cx2018022).

REFERENCES

(1). Li, X. W.; Li, J.; Van Der Werff, H. *Flora of China* (*Zhongguo Zhiwu Zhi*). Science Press: Beijing, China, 2008. Vol. 7, pp. 166–187.

(2). Lee, H.-S.; Kim, B.-S.; Kim M.-K. Suppression effect of *Cinnamomum cassia* bark-derived component on nitric oxide synthase. *J. Agric. Food Chem.* **2002**, *50*, 7700–7703.

(3). Jayaprakasha, G. K.; Rao, L. J. M.; Sakariah, K. K. Volatile constituents from *Cinnamomum zeylanicum* fruit stalks and their antioxidant activities. *J. Agric. Food Chem.* **2003**, *51*, 4344–4348.

(4). Chericoni, S.; Prieto, J. M.; Iacopini, P.; Cioni, P.; Morelli, I. In vitro activity of the essential oil of *Cinnamomum zeylanicum* and eugenol in peroxynitrite-induced oxidative processes. *J. Agric. Food Chem.* **2005**, *53*, 4762–4765.

(5). Jayaprakasha, G. K.; Ohnishi-Kameyama, M.; Ono, H.; Yoshida, M.; Rao, L. J. M. Phenolic constituents in the fruits of *Cinnamomum zeylanicum* and their antioxidant activity. *J. Agric. Food Chem.* **2006**, *54*, 1672–1679.

(6). Killday, K. B.; Davey, M. H.; Glinski, J. A.; Duan, P.; Veluri, R.; Proni, G.; Daugherty, F. J.; Tempesta, M. S. Bioactive a-type proanthocyanidins from *Cinnamomum cassia*. *J. Nat. Prod.* **2011**, *74*, 1833–1841.

(7). Zeng, J.; Xue, Y.; Shu, P.; Qian, H.; Sa, R.; Xiang, M.; Li, X.-N.; Luo, Z.; Yao, G.; Zhang, Y. Diterpenoids with immunosuppressive activities from *Cinnamomum cassia*. *J. Nat. Prod.* **2014**, *77*, 1948–1954.

(8). Guoruoluo, Y.; Zhou, H.; Zhou, J.; Zhao, H.; Aisa, H. A.; Yao, G. Isolation and characterization of sesquiterpenoids from cassia buds and their antimicrobial activities. *J. Agric. Food Chem.* **2017**, *65*, 5614–5619.

(9). Chao, L. K.; Hua, K.-F.; Hsu, H.-Y.; Cheng, S.-S.; Liu, J.-Y.; Chang, S.-T. Study on the antiinflammatory activity of essential oil from leaves of *Cinnamomum osmophloeum*. *J. Agric. Food Chem.* **2005**, *53*, 7274–7278.

(10). Marongiu, B.; Piras, A.; Porcedda, S.; Tuveri, E.; Sanjust, E.; Meli, M.; Sollai, F.; Zucca, P.; Rescigno, A. Supercritical CO_2 extract of *Cinnamomum zeylanicum*: chemical characterization and antityrosinase activity. *J. Agric. Food Chem.* **2007**, *55*, 10022–10027.

(11). Tung, Y.-T.; Huang, C.-C.; Ho, S.-T.; Kuo, Y.-H.; Lin, C.-C.; Lin, C.-T.; Wu, J.-H. Bioactive phytochemicals of leaf essential oils of *Cinnamomum osmophloeum* prevent lipopolysaccharide/D-galactosamine (LPS/D-GalN)-induced acute hepatitis in mice. *J. Agric. Food Chem.* **2011**, *59*, 8117–8123.

(12). Hsu, F.-L.; Li, W.-H.; Yu, C.-W.; Hsieh, Y.-C.; Yang, Y.-F.; Liu, J.-T.; Shih, J.; Chu, Y.-J.; Yen, P.-L.; Chang, S.-T.; Liao, V. H.-C. In vivo antioxidant activities of essential oils and their constituents from leaves of the taiwanese *Cinnamomum osmophloeum*. *J. Agric. Food Chem.* **2012**, *60*, 3092–3097.

(13). Lee, S.-C.; Xu, W.-X.; Lin, L.-Y.; Yang, J.-J.; Liu, C.-T. Chemical composition and hypoglycemic and pancreas-protective effect of leaf essential oil from indigenous cinnamon (*Cinnamomum osmophloeum* Kanehira). *J. Agric. Food Chem.* **2013**, *61*, 4905–4913.

(14). Wang, H.-M.; Chiu, C.-C.; Wu, P.-F.; Chen, C.-Y. Subamolide E from *Cinnamomum subavenium* induces Sub-G1 cell-cycle arrest and caspase-dependent apoptosis and reduces the migration ability of human melanoma cells. *J. Agric. Food Chem.* **2011**, *59*, 8187–8192.

(15). Lin, R.-J.; Cheng, M.-J.; Huang, J.-C.; Lo, W.-L.; Yeh, Y.-T.; Yen, C.-M.; Lu, C.-M.; Chen, C.-Y. Cytotoxic compounds from the stems of *Cinnamomum tenuifolium*. *J. Nat. Prod.* **2009**, *72,* 1816–1824.

(16). Guoruoluo, Y.; Zhou, H.; Wang, W.; Zhou, J.; Aisa, H. A.; Yao, G. Chemical constituents from the immature buds of *Cinnamomum cassia* (Lauraceae). *Biochem. Syst. Ecol* **2018**, *78*, 102−105.

(17). Ngoc, T. M.; Lee, I. S.; Ha, D. T.; Kim, H. J.; Min, B. S.; Bae, K. H. Tyrosinase-inhibitory constituents from the twigs of *Cinnamomum cassia*. *J. Nat. Prod.* **2009**, *72*, 1205–1208.

(18). Shu, P.; Wei, X.; Xue, Y.; Li, W.; Zhang, J.; Xiang, M.; Zhang, M.; Luo, Z.; Li, Y.; Yao, G.; Zhang, Y. Wilsonols A−L, megastigmane sesquiterpenoids from the leaves of *Cinnamomum wilsonii*. *J. Nat. Prod.* **2013**, *76*, 1303–1312.

(19). Zhou, H.; Guoruoluo, Y.; Tuo, Y.; Zhou, J.; Zhang, H.; Wang, W.; Xiang, M.; Aisa, H. A.; Yao, G. Cassiabudanols A and B, immunostimulative diterpenoids with a cassiabudane carbon skeleton featuring a 3-oxatetracyclo[6.6.1.$0^{2,6}$.$0^{10,14}$]pentadecane scaffold from cassia buds. *Org. Lett.* **2019**, *21*, 549–553.

(20). Zhou, L.; Tuo, Y.; Hao, Y.; Guo, X.; Tang, W.; Xue, Y.; Zeng, J.; Zhou, Y.; Xiang, M.; Zuo, J.; Yao, G.; Zhang, Y. Cinnamomols A and B, immunostimulative diterpenoids with a new carbon skeleton from the leaves of *Cinnamomum cassia*. *Org. Lett.* **2017**, *19*, 3029–3032.

(21). Lai, Y.; Liu, T.; Sa, R.; Wei, X.; Xue, Y.; Wu, Z.; Luo, Z.; Xiang, M.; Zhang, Y.; Yao, G. Neolignans with a rare 2-oxaspiro[4.5]deca-6,9-dien-8-one motif from the stem bark of *Cinnamomum subavenium*. *J. Nat. Prod.* **2015**, *78*, 1740–1744.

(22). Liu, X.; Fu, J.; Yao, X.-J.; Yang, J.; Liu, L.; Xie, T.-G.; Jiang, P.-C.; Jiang, Z.-H.; Zhu, G.-Y. Phenolic constituents isolated from the twigs of *Cinnamomum cassia* and their potential neuroprotective effects. *J. Nat. Prod.* **2018**, *81*, 1333–1342.

(23). Baruah, A.; Nath, S. C.; Hazarika, A. K.; Sarma, T. C.; Essential oils of the leaf, stem bark and panicle of *Cinnamomum bejolghota* (Buch.-Ham.). *J. Essent. Oil Res.* **1997**, *9*, 243–245.

(24). Choudhury, S.; Ahmed, R.; Barthel, A.; Leclercq, P. A. Composition of the bark and flower oils of *Cinnamomum bejolghota* (Buch.-Ham.) Sweet from two locations of Assam, India. *J. Essent. Oil Res.* **1998**, *10*, 245–250.

(25). Atiphasaworn, P.; Monggoot, S.; Pripdeevech, P. Chemical composition, antibacterial and antifungal activities of *Cinamomum bejolghota* bark oil from Thailand. *J. Applied Pharm. Sci.* **2017**, *7*, 69–73.

(26). Gogoi, B.; Kakoti, B. B.; Borah, S.; Borah, N. S. Antihyperglycemic and in vivo antioxidative activity evaluation of *Cinnamomum bejolghota* (Buch.-Ham.) in streptozotocin induced diabetic rats: an ethnomedicinal plant in Assam. *Asian Pac. J. Trop. Med.* **2014**, *7*, 427–434.

(27). Blois, M. S. Antioxidant determinations by the use of a stable free radical. *Nature* **1958**, *181*, 1199–1200.

(28). Fan, Y.; Liu, Y.; You, Y.-X.; Rao, L.; Su, Y.; He, Q.; Hu, F.; Li, Y.; Wei, W.; Xu, Y.-K.; Lin, B.; Zhang, C.-R. Cytotoxic arylalkenyl α,*β*-unsaturated *δ*-lactones from *Cryptocarya brachythyrsa*. *Fitoterapia* **2019**, *136*, 104167.

(29). Jiang, C.; Luo, P.; Zhao, Y.; Hong, J.; Morris-Natschke, S. L.; Xu, J.; Chen, C.-H.; Lee, K.-H.; Gu, Q. Carolignans from the aerial parts of *Euphorbia sikkimensis* and their anti-HIV activity. *J. Nat. Prod.* **2016**, *79*, 578–583.

548 (30). Seca, A. M. L.; Silva, A. M. S.; Silvestre, A. J. D.; Cavaleiro, J. A. S.; Domingues, F. M.
549 J.; Pascoal-Neto, C. Phenolic constituents from the core of Kenaf (*Hibiscus cannabinus*).
550 *Phytochemistry* **2001**, *56*, 759–767.
551 (31). Zhu, J.-Y.; Cheng, B.; Zheng, Y.-J.; Dong, Z.; Lin, S.-L.; Tang, G.-H.; Gu Q.; Yin, S.
552 Enantiomeric neolignans and sesquineolignans from *Jatropha integerrima* and their absolute
553 configurations. *RSC Adv.* **2015**, *5*, 12202–12208.
554 (32). Becke, A. D. Density-functional exchange-energy approximation with correct asymptotic
555 behavior. *Phys. Rev. A* **1998**, *38*, 3098−3100.
556 (33). Lee, C.; Yang, W. T.; Parr, R. G. Development of the Colie-Salvetti correlation-energy
557 formula into a functional of the electron density. *Phys. Rev. B* **1998**, *37*, 785−789.
558 (34). York, D. M.; Karplus, M. A smooth solvation sotential based on the conductor-like
559 screening model. *J. Phys. Chem. A* **1999**, *103*, 11060−11079.
560 (35). Chen, T.-H.; Huang, Y.-H.; Lin, J.-J.; Liau, B.-C.; Wang, S.-Y.; Wu, Y.-C.; Jong, T.-T.
561 Cytotoxic lignan esters from *Cinnamomum osmophloeum*. *Planta Med.* **2010**, *76*, 613–619.
562 (36). Gu, H. S.; Ma, S. G.; Li, L.; Qu, J.; Liu, Y. B.; Yu, S. S. Diketopiperazines and
563 sesquilignans from the branches and leaves of *Claoxylon polot*. *Planta Med.* **2015**, *81*, 748–753.
564 (37). Liu, Q.-B.; Huang, X.-X.; Bai, M.; Chang, X.-B.; Yan, X.-J.; Zhu, T.; Zhao, W.; Peng,
565 Y.; Song, S.-J. Antioxidant and anti-inflammatory active dihydrobenzofuran neolignans from the
566 seeds of *Prunus tomentosa*. *J. Agric. Food Chem.* **2014**, *62*, 7796–7803.
567 (38). Matsutomo, T.; Stark, T. D.; Hofmann, T. In vitro activity-guided identification of
568 antioxidants in aged garlic extract. *J. Agric. Food Chem.* **2013**, *61*, 3059–3067.

569 (39). Zhu, J. X.; Ren J.; Qin, J. J.; Chen, X. R.; Zeng, Q.; Zhang, F.; Yan, S. K.; Jin, H. Z.;
570 Zhang, W. D. Phenylpropanoids and lignanoids from *Euonymus acanthocarpus*. *Arch. Pharm.*
571 *Res.* **2012**, *35*, 1739–1747.
572 (40). Xiong, L.; Zhu, C.; Li, Y.; Tian, Y.; Lin, S.; Yuan, S.; Hu, J.; Hou, Q.; Chen, N.; Yang,
573 Y.; Shi, J. Lignans and neolignans from *Sinocalamus affinis* and their absolute configurations. *J.*
574 *Nat. Prod* **2011**, *74*, 1188–1200.
575 (41). Dong, L.-M.; Jia, X.-C.; Luo, Q.-W.; Zhang, Q.; Luo, B.; Liu, W.-B.; Zhang, X.; Xu, Q.-
576 L.; Tan, J.-W. Phenolics from Mikania micrantha and their antioxidant activity. *Molecules* 2017,
577 *22*, 1140.
578 (42). Bai, Ming.; Li, S.-F.; Liu, S.-F.; Wang, X.-B.; Huang, X.-X.; Song, S.-J. Iridoid
579 glycoside and lignans from a wild vegetable (*Patrinia villosa* Juss.) with antioxidant activity. *J.*
580 *Food Biochem.* **2018**, *42*, e12521.
581 (43). Li, X.; Cao, W.; Shen, Y.; Li, N.; Dong, X.-P.; Wang, K.-J.; Cheng, Y.-X. Antioxidant
582 compounds from *Rosa laevigata* fruits. *Food Chem.* **2012**, *130*, 575–580.
583 (44). Huang, X.-X.; Zhou, C.-C.; Li, L.-Z.; Li, F.-F.; Lou, L.-L.; Li, D.-M. The cytotoxicity of
584 8-O-4′ neolignans from the seeds of *Crataegus pinnatifida*. *Bioorg. Med. Chem. Lett.* **2013**, *23*,
585 5599–5604.
586 (45). Yang, X.-W.; Zhao, P.-J.; Ma, Y.-L.; Xiao, H.-T.; Zuo, Y.-Q.; He, H.-P.; Li, L.; Hao, X.-
587 J. Mixed lignan-neolignans from *Tarenna attenuata*. *J. Nat. Prod.* **2007**, *70*, 521–525.
588 (46). Zhao, C.; Chen, J.; Shao, J.; Shen, J.; Li, K.; Gu, W.; Li, S.; Fan, J. Neolignan
589 constituents with potential beneficial effects in prevention of type 2 diabetes from *Viburnum*
590 *fordiae* Hance fruits. *J. Agric. Food Chem.* **2018**, *66*, 10421–10430.

591 **Figure Captions**

592 **Figure 1.** Structures of pure isolates **1**–**21** from *Cinnamomum bejolghota*.

593 **Figure 2.** ^{1}H–^{1}H COSY (▬), Selected HMBC (H→C) and ROESY (H↔H) correlations of **1**

594 (A), **9** (B) and **11** (C).

595 **Figure 3.** Experimental and calculated ECD spectra of **1**−**4** and **9**−**11.**

Table 1. ^{1}H and ^{13}C NMR Data for Compounds 1−4 in $CDCl_3$

no.	1		2		3		4	
	δ_H (mult, *J* in Hz)	δ_C	δ_H (mult, *J* in Hz)	δ_C	δ_H (mult, *J* in Hz)	δ_C	δ_H (mult, *J* in Hz)	δ_C
1		137.9		137.7		137.6		137.7
2	6.69 (s)	103.3	6.67 (s)	103.2	6.63 (s)	103.0	6.66 (s)	103.4
3		153.7		153.7		152.9		153.7
4		134.4		134.5		136.3		134.5
5		153.7		153.7		152.9		153.7
6	6.69 (s)	103.3	6.67 (s)	103.2	6.63 (s)	103.0	6.66 (s)	103.4
7	5.58 (d, 7.3)	87.9	5.61 (d, 6.9)	88.2	5.58 (d, 7.0)	88.2	5.61 (d, 6.3)	88.2
8	3.62 (brd, 5.4)	54.0	3.62 (brd, 4.9)	53.8	3.57 (dd, 11.6, 5.7)	53.9	3.62 (m)	53.8
9a	3.98 (dd, 11.0, 6.0)	64.1	3.97 (dd, 11.0, 6.3)	64.2	3.94 (2H, m)[a]	64.2	3.95 (2H, m)[a]	64.2
9b	3.93 (dd, 11.0, 4.7)		3.93 (dd, 11.0, 4.6)					
1′		135.9		131.3		131.3		131.3
2′	6.67 (s)	116.0	6.87 (s)	114.8	6.87 (s)	114.9	6.89 (s)	114.9
3′		127.5		127.9		128.0		127.9
4′		146.7		148.3		148.3		148.3
5′		144.4		144.6		144.6		144.6
6′	6.69 (s)	112.6	6.88 (s)	110.6	6.88 (s)	110.7	6.89 (s)	110.7
7′	2.68 (2H, t, 7.6)	32.2	6.55 (d, 15.8)	131.3	6.56 (d, 15.8)	131.3	6.56 (d, 15.8)	131.3
8′	1.89 (2H, m)	34.8	6.24 (m)[a]	126.8	6.24 (dt, 15.8, 5.9)	126.8	6.24 (dt, 15.8, 5.8)	126.8
9′	3.70 (2H, t, 6.2)	62.4	4.30 (2H, d, 6.0)	63.9	4.31 (2H, d, 5.4)	63.9	4.31 (d, 5.5)	63.9
1″		130.8		130.8		131.8		130.8
2″	6.99 (d, 1.8)	108.6	6.99 (s)	108.6	6.86 (s)	109.4	6.96 (s)	108.6
3″		146.6		146.7		146.6		146.7
4″		144.9		144.9		145.5		144.9
5″	6.91 (dd, 8.1, 1.8)	114.3	6.86 (m)[a]	114.3	6.82 (d, 8.3)	114.4	6.84 (m)[a]	114.3
6″	6.77 (d, 8.1)	119.0	6.76 (d, 8.3)	118.9	6.85 (m)[a]	120.2	6.75 (m)[a]	119.0
7″	4.87 (brs)	71.7	4.87 (brs)	71.8	5.07 (d, 8.0)	74.2	4.83 (brs)	71.8
8″	4.55 (m)	83.4	4.54 (m)	83.4	4.12 (m)	86.8	4.49 (m)[a]	83.6
9″a	4.45 (dd, 11.9, 7.6)	62.6	4.45 (dd, 11.9, 7.6)	62.6	4.53 (ddd, 22.6, 12.1, 3.2)	63.9	4.46 (m)[a]	62.6
9″b	4.33 (dd, 11.9, 3.6)		4.32 (dd, 11.9, 3.6)		4.05 (dt, 12.1, 3.2)		4.18 (dd, 11.7, 2.5)	
1‴		127.2		127.1		127.0		127.3
2‴	7.00 (s)	109.4	6.99 (s)	109.4	7.05 (s)	109.4	7.75 (s)	113.0
3‴		146.9		146.9		147.0		146.0
4‴		148.1		148.1		148.2		147.2
5‴	6.90 (d, 8.1)	114.8	6.89 (m)[a]	114.8	6.92 (m)[a]	114.9	6.83 (m)[a]	113.9
6‴	7.02 (d, 8.1)	123.2	7.01 (d, 8.2)	123.2	7.06 (m)[a]	123.4	7.08 (d, 8.0)	126.0
7‴	7.50 (d, 15.9)	144.8	7.49 (d, 15.9)	144.9	7.56 (t, 15.8)	145.2	6.74 (d, 12.8)	144.0
8‴	6.23 (d, 15.9)	115.7	6.22 (d, 15.9)	115.6	6.34 (d, 15.8)	115.3	5.74 (d, 12.8)	116.6
9‴		167.1		167.2		167.1		166.3
4″-OH	5.54 (s)		5.59 (s)		5.59 (s)		5.59 (m)[a]	
7″-OH	4.21 (d, 7.9)		4.21 (brs)		4.64 (dd, 9.7, 1.8)		4.20 (s)[a]	
4‴-OH	5.87 (s)		5.94 (s)		5.93 (s)		5.92 (s)	
3-OMe	3.83 (s)	56.4	3.82 (s)	56.4	3.83 (s)	56.2	3.80 (s)	56.4
5-OMe	3.83 (s)	56.4	3.82 (s)	56.4	3.83 (s)	56.2	3.80 (s)	56.4
5′-OMe	3.89 (s)	56.1	3.91 (s)	56.1	3.91 (s)	56.2	3.91 (s)	56.1
3″-OMe	3.89 (s)	56.1	3.88 (s)	56.1	3.82 (s)	56.2	3.86 (s)	56.1
3‴-OMe	3.92 (s)	56.1	3.91 (s)	56.1	3.94 (s)	56.2	3.85 (s)	56.1

[a]overlapped

Table 2. ^{1}H and ^{13}C NMR Data for Compounds 9–11 in $CDCl_3$

no.	9		10		11	
	δ_H (mult, J in Hz)	δ_C	δ_H (mult, J in Hz)	δ_C	δ_H (mult, J in Hz)	δ_C
1		132.3		134.6		128.8
2	6.68 (s)	111.3	6.60 (s)	102.9	6.50 (s)	106.1
3		146.7		147.4		146.4
4		144.2		134.2		137.2
5	6.84 (d, 8.2)	114.6		147.4		145.6
6	6.69 (d, 8.2)	121.3	6.60 (s)	102.9		124.8
7a	2.90 (dd, 13.5, 5.2)	33.4	4.92 (d, 5.9)	73.0	2.74 (m, 2H)	32.8
7b	2.56 (dd, 13.5, 10.7)					
8	2.72 (m)	42.6	2.88 (m)	47.5	1.85 (m)	39.3
9a	4.07 (brt, 7.6)	73.3	4.23 (brt, 7.8)	69.6	3.73 (dd, 10.4, 3.6)	65.9
9b	3.76 (dd, 8.1, 7.2)		4.16 (dd, 8.8, 7.5)		3.67 (dd, 10.4, 5.9)	
1′		139.8		134.5		137.8
2′	6.60 (s)	102.8	6.59 (s)	102.8	6.34 (s)	105.2
3′		153.6		147.2		147.0
4′		133.7		133.6		133.1
5′		153.6		147.2		147.0
6′	6.60 (s)	102.8	6.59 (s)	102.8	6.34 (s)	105.2
7′	4.85 (d, 5.9)	83.1	4.91 (d, 6.3)	84.4	4.27 (d, 6.3)	42.5
8′	2.41 (brt, 6.6)	52.6	2.53 (m)	48.7	2.24 (m)	44.7
9′a	3.93 (m)[a]	61.1	4.60 (dd, 11.3, 5.9)	63.0	4.30 (dd, 11.4, 3.8)	65.2
9′b	3.80 (m)[a]		4.37 (dd, 11.3, 7.7)		4.17 (dd, 11.4, 5.1)	
1″		130.9		126.8		127.0
2″	7.02 (s)	108.6	6.98 (d, 1.5)	109.6	7.02 (s)	109.4
3″		146.7		147.0		146.9
4″		144.9		148.4		148.2
5″	6.87 (d, 8.1)	114.2	6.92 (d, 8.2)	115.0	6.91 (d, 8.1)	114.9
6″	6.77 (d, 8.1)	118.9	7.04 (dd, 8.2, 1.5)	123.2	7.05 (d, 8.1)	123.4
7″	4.89 (brs)	71.7	7.47 (d, 15.9)	145.6	7.59 (d, 16.0)	145.4
8″	4.56 (m)	83.3	6.19 (d, 15.9)	114.9	6.29 (d, 16.0)	115.3
9″a	4.46 (dd, 11.8, 7.5)	62.6		167.1		167.5
9″b	4.32 (dd, 11.8, 3.7)					
1‴		127.2				
2‴	7.01 (s)	109.4				
3‴		146.9				
4‴		148.1				
5‴	6.90 (d, 8.1)	114.8				
6‴	7.03 (d, 8.1)	123.2				
7‴	7.51 (d, 15.9)	144.8				
8‴	6.24 (d, 15.9)	115.7				
9‴		167.2				
4-OH	5.51 (s)		5.44 (s)		5.36 (s)	
4′-OH			5.49 (s)		5.36 (s)	
4″-OH	5.55 (s)		5.88 (s)		5.90 (s)	
7″-OH	4.26 (d, 9.8)					
4‴-OH	5.87 (s)					
3-OMe	3.86 (s, 3H)	56.1	3.88 (s, 3H)	56.6	3.90 (s, 3H)	56.3
5-OMe			3.88 (s, 3H)	56.6	3.36 (s, 3H)	59.9
3′-OMe	3.85 (s, 3H)	56.4	3.87 (s, 3H)	56.5	3.78 (s, 3H)	56.6
5′-OMe	3.85 (s, 3H)	56.4	3.87 (s, 3H)	56.5	3.78 (s, 3H)	56.6
3″-OMe	3.89 (s, 3H)	56.1	3.95 (s, 3H)	56.2	3.93 (s, 3H)	56.1
3‴-OMe	3.92 (s, 3H)	56.1				

Table 3. DPPH Free Radical Scavenging Activity of 1–21 and Positive Controls

Comp.	IC_{50} (μM)	Comp.	IC_{50} (μM)	Comp.	IC_{50} (μM)
1	37.8 ± 1.9	**9**	35.2 ± 0.5	**17**	32.2 ± 1.4
2	34.4 ± 1.8	**10**	34.2 ± 2.5	**18**	33.7 ± 2.1
3	38.5 ± 0.2	**11**	22.8 ± 1.7	**19**	38.3 ± 2.2
4	35.4 ± 1.1	**12**	23.7 ± 0.9	**20**	30.1 ± 1.9
5	24.6 ± 2.5	**13**	31.1 ± 2.1	**21**	35.4 ± 0.8
6	26.9 ± 1.3	**14**	45.1 ± 2.3	Ascorbic acid	25.2 ± 1.4
7	49.5 ± 1.4	**15**	44.3 ± 1.4	BHT	23.3 ± 1.7
8	46.9 ± 1.8	**16**	> 100		

Table 4. Human Cancer Cell Proliferation Inhibition of 1–3, 11–13 and Positive Control

Comp.	IC_{50} (μM)				
	HCT-116	A549	MDA-MB-231	BEAS-2B	L02
1	39.9 ± 0.41	36.9 ± 0.31	45.6 ± 0.51	> 100	> 100
2	35.2 ± 0.53	40.7 ± 0.47	44.6 ± 0.25	> 100	> 100
3	27.8 ± 0.25	39.9 ± 0.33	18.5 ± 0.31	> 100	> 100
11	1.97 ± 0.13	2.93 ± 0.25	2.71 ± 0.17	> 100	> 100
12	1.43 ± 0.15	2.79 ± 0.11	2.43 ± 0.13	> 100	> 100
13	0.78 ± 0.09	0.86 ± 0.15	0.83 ± 0.07	> 100	> 100
Adriamycin	0.16 ± 0.01	0.29 ± 0.02	0.18 ± 0.02	0.79 ± 0.05	0.92 ± 0.08

Figure1

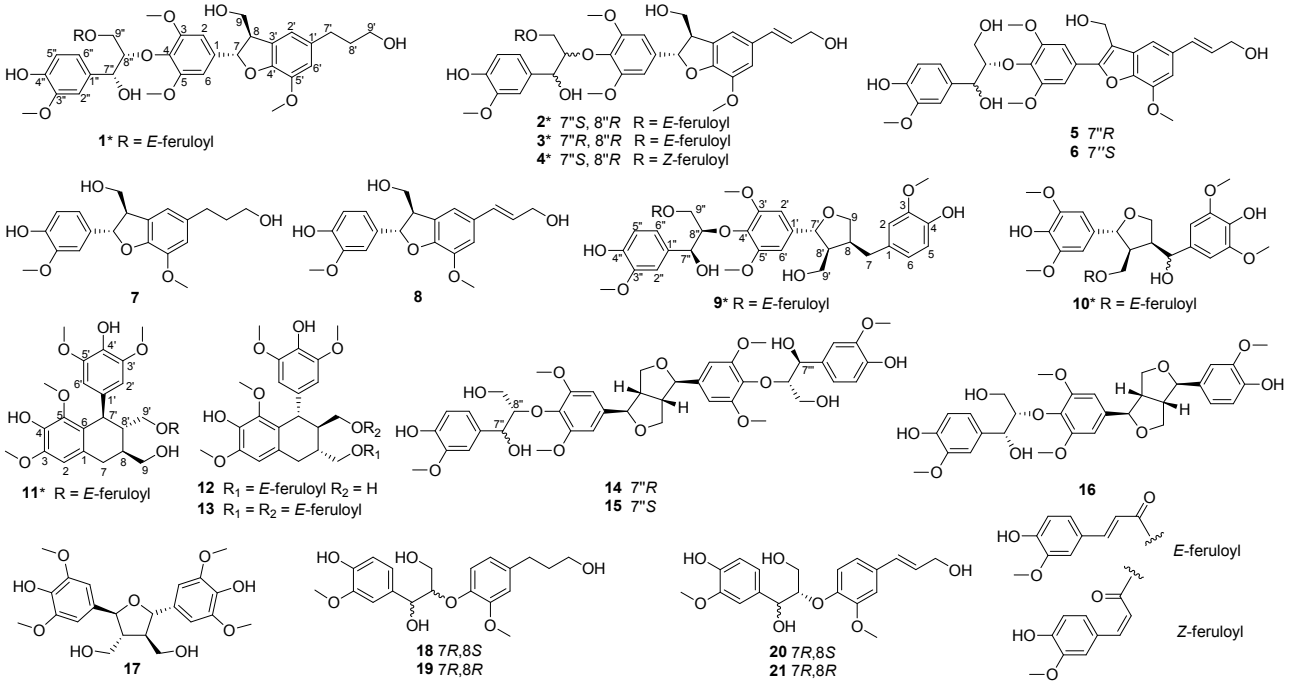

Figure 2

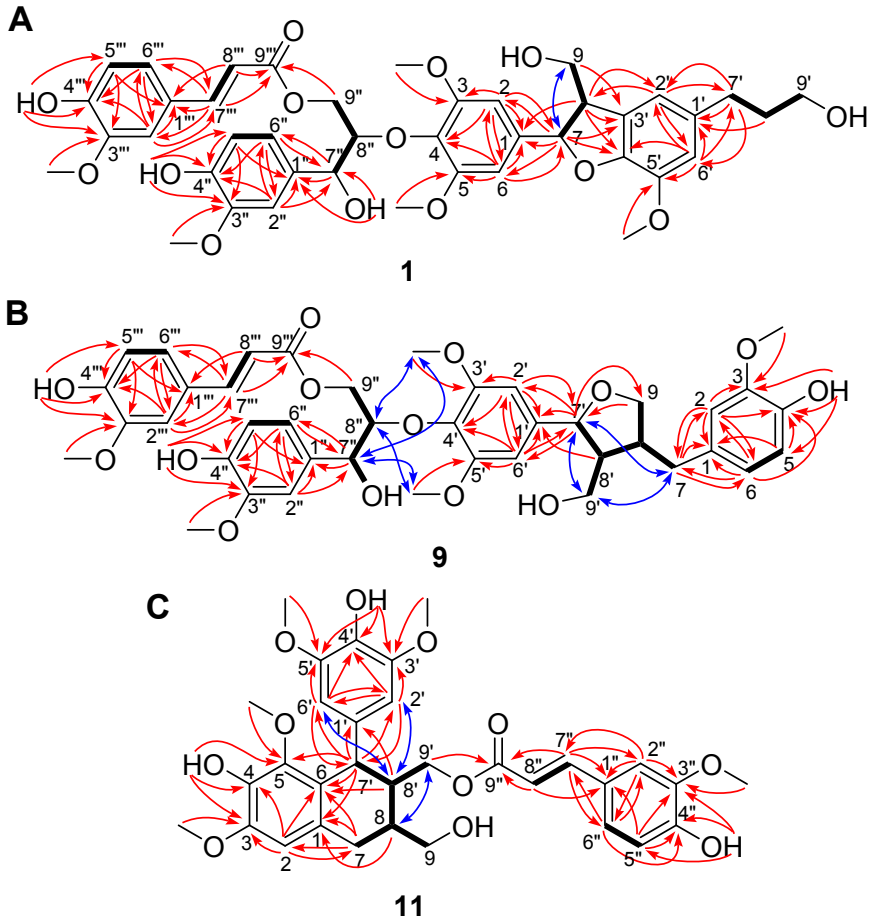

Figure 3

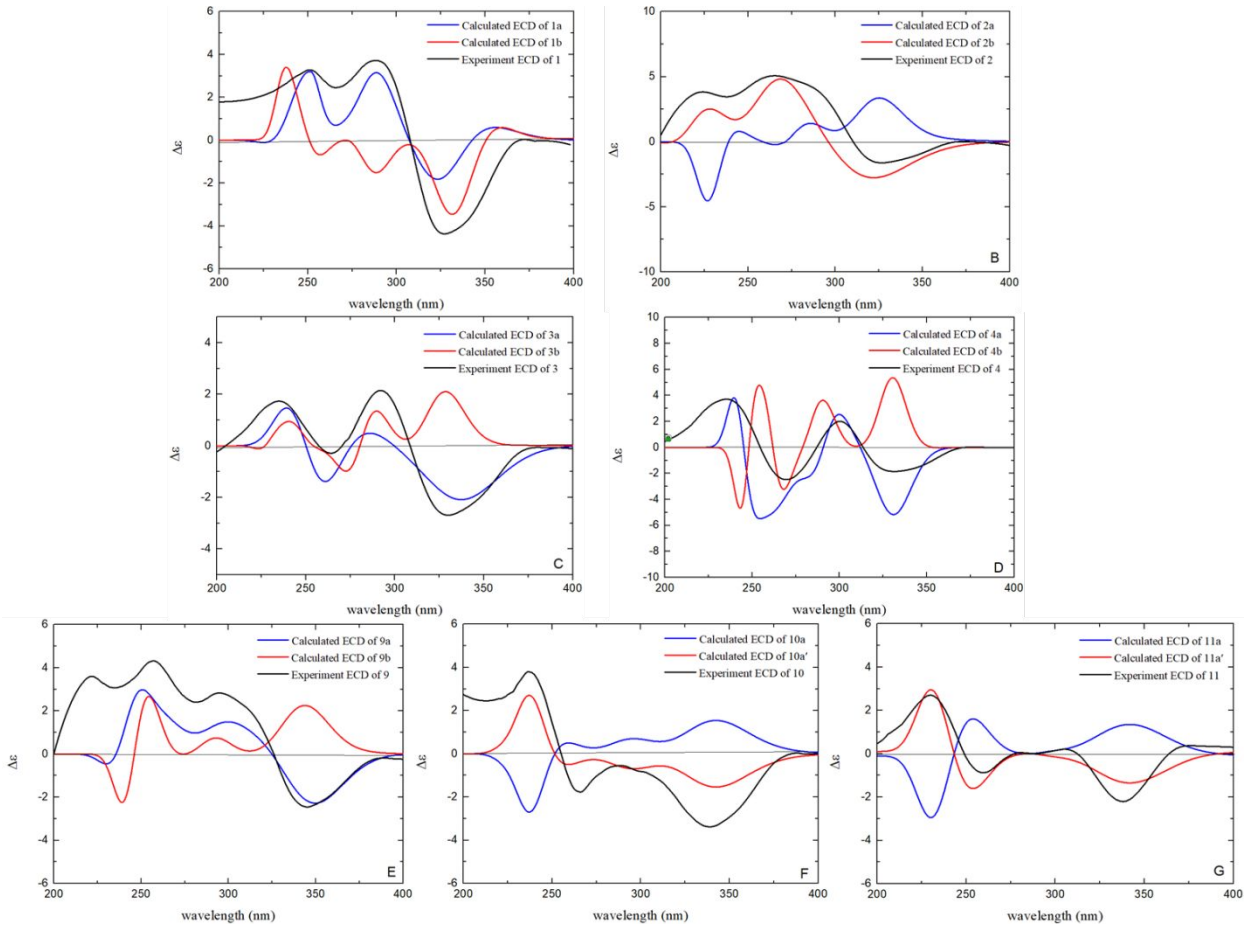
Calculated ECD of 1a
Calculated ECD of 1b
Experiment ECD of 1
Calculated ECD of 2a
Calculated ECD of 2b
Experiment ECD of 2
Calculated ECD of 3a
Calculated ECD of 3b
Experiment ECD of 3
Calculated ECD of 4a
Calculated ECD of 4b
Experiment ECD of 4
Calculated ECD of 9a
Calculated ECD of 9b
Experiment ECD of 9
Calculated ECD of 10a
Calculated ECD of 10a'
Experiment ECD of 10
Calculated ECD of 11a
Calculated ECD of 11a'
Experiment ECD of 11
Δε
wavelength (nm)
B
C
D
E
F
G

Table of Contents/Abstract Graphics